General Disclaimer

One or more of the Following Statements may affect this Document

- This document has been reproduced from the best copy furnished by the organizational source. It is being released in the interest of making available as much information as possible.

- This document may contain data, which exceeds the sheet parameters. It was furnished in this condition by the organizational source and is the best copy available.

- This document may contain tone-on-tone or color graphs, charts and/or pictures, which have been reproduced in black and white.

- This document is paginated as submitted by the original source.

- Portions of this document are not fully legible due to the historical nature of some of the material. However, it is the best reproduction available from the original submission.

X-692-76-168

PREPRINT

INTERPLANETARY BOUNDARY LAYERS AT 1 A. U.

L. F. BURLAGA
J. F. LEMAIRE
J. M. TURNER

JULY 1976

GSFC
GODDARD SPACE FLIGHT CENTER
GREENBELT, MARYLAND

INTERPLANETARY BOUNDARY LAYERS AT 1 A. U.

L. F. Burlaga *

J. F. Lemaire †

J. M. Turner +

* NASA/Goddard Space Flight Center, Laboratory for Extraterrestrial Physics, Greenbelt, MD 20771.

† Institut d'Aeronomie Spatiale, 3, Avenue Circulaire, B-1180 Brussels, Belgium.

+ Department of Physics, Morehouse College, Atlanta, GA 30314.

ABSTRACT

We have determined the structure and nature of "discontinuities" in the interplanetary magnetic field at 1 AU in the period March 18, 1971 to April 9, 1971, by using high-resolution magnetic field measurements from Explorer 34. The discontinuities that were selected for this analysis occurred under a variety of interplanetary conditions at an average rate of 0.5/hr. This set does not include all discontinuities that were present, but the sample is large and it is probably representative. Both tangential and rotational discontinuities were identified, the ratio of TD's to RD's being approximately 3 to 1. Tangential discontinuities were observed every day, even among Alfvénic fluctuations. In particular, on one day during which Alfvénic fluctuations were intense and persistent in a high-speed stream, tangential discontinuities were seen throughout the day at an average rate of 0.5/hr; rotational discontinuities were also observed during this day, at a higher than usual rate, the ratio of TD's to RD's being approximately one. The structure of most of the boundary layers was simple and ordered, i.e., the magnetic field usually changed smoothly and monotonically from one side of the boundary layer to the other. The thickness distributions of the TD's and RD's with very smooth boundary layers were similar. The average thickness of the RD's was 1,200 km (13 proton Larmor radii), and the average thickness of the TD's was 1,300 km (12 proton Larmor radii).

1. Introduction

The nature and structure of interplanetary discontinuities have been the subject of several investigations and much debate. Siscoe et al. (1968) used a minimum variance method to examine the structure of boundary layers whose width ranged from 10s to 100 sec, and they concluded that 80% seemed to be TD's; however, the method they used is not appropriate for studying RD's, and they could not rule out a substantial contribution of RD's. Burlaga (1971) showed that during an 8-day period (when there were no pronounced high-speed streams), less than 25% of the directional discontinuities were RD's, and he concluded that those discontinuities were predominantly TD's. The predominance of TD's in quiet, low-speed regions has been confirmed by Martin et al. (1973) and Solodyna et al. (1976). Belcher and Solodyna (1975) showed that the condition

$$\delta\underset{\sim}{V} = \pm (V/B)\ \delta\underset{\sim}{B} \qquad (1)$$

is nearly satisfied across discontinuities that occur among Alfvénic fluctuations in high-speed regions, and this led them to the opinion that such discontinuities are predominantly rotational. Martin et al. (1973) arrived at the same opinion in the same way. However, (1) is not a sufficient condition for an RD. Indeed, Denskat and Burlaga (1976) have shown, using plasma and magnetic field observations from two spacecraft, that there do exist TD's across which (1) is satisfied. Thus, in order to identify the nature of the discontinuities in "Alfvénic", high-speed regions one must do more than test for (1). Smith (1973a) examined the structure of some 'discontinuities', and he found a distribution consistent with the presence of both TD's and RD's. However, he considered only a small fraction of the discontinuities that were present (118

discontinuities in 39 days, or 3/day); he selected only exceptionally broad current sheets; and he did not consider plasma data.

The Explorer 43 magnetic field measurements that we use in this paper clearly resolve the structure of even the thinnest boundary layers, and the measurement errors are small enough that we can determine the nature of most of the associated discontinuities using a minimum variance method. This is done in Section 3. Since we have plasma data for the period considered, we can also examine the relation between these discontinuities and Alfvénic fluctuations, and we do this in Section 4. Finally, since the structure of the current sheets is resolved in the Explorer 43 data, we can determine the distribution of thickness for all events with a well-defined beginning and end; we present those results in Section 5.

The plasma and magnetic field instruments are described briefly by Burlaga and Ogilvie (1973) and Fairfield (1974), respectively.

2. Selection of Discontinuities

The discontinuities were selected subjectively by looking at plots of 1.28 sec averages of the magnetic field (B (t), θ (t), ϕ (t)) on a scale of $\approx$ 1 hour/20 inches. Essentially, events were selected because they looked like abrupt changes in the time profile of the magnetic field direction, i.e., the direction changed from one nearly uniform state to another in less than $\approx$ 30 sec. The selection was made independently by four people (L. Burlaga, J. Chao, D. Fairfield, and N. Ness), and there was general agreement as to which events were to be chosen.

Examples of the kinds of discontinuities that were selected for this study are shown in Figures 1 and 2. Figure 1 shows a discontinuity at which the change in direction, ω, is relatively large ($\omega = 75^{\circ}$) and which stands alone in a 10 min. interval; this event satisfies the definition of a directional discontinuity introduced by Burlaga (1969). Figure 2 shows several discontinuities at which the change in direction is small and which are clustered in a 5 min. interval; events such as these do not satisfy the definition of directional discontinuities, but we included them initially, because they can be readily identified in the high-resolution Explorer 43 data.

Our selection procedure gave 287 discontinuities for this study, from 430 hours during which plasma measurements were made in the period March 18, 1971 to April 9, 1971. Thus, the rate of occurrence is 0.7/hr. This may be compared with the occurrence rate for directional discontinuities that was found in other studies (see Siscoe, 1976; Burlaga 1972), viz. $\approx$ 1/hr. Our selection procedure did not identify all of the directional discontinuities that were present. Conversely, 31% of the events that we selected were not

directional discontinuitie the sense that the angle, ω, between the field $\underset{\sim}{B}_1$ on one side of the ntinuity and the field $\underset{\sim}{B}_2$ on the other side was less than 30° ($\omega < 30^\circ$). In other words, although we did not select all discontinuities, we do have a large and representative sample of discontinuities.

The distribution of ω for the discontinuities that were sele ted is shown in Figure 3. One can see that there were 95 events witn $\omega < 30^\circ$. The number of events with $\omega > 30^\circ$ falls off exponentially with ω^2, as shown by the dashed curve in Figure 3. This is the same curve that Burlaga (1969) obtained for directional discontinuities in the Pioneer 6 data, viz. $N = \text{constant} \times \exp(-\omega/75^\circ)^2$. It describes the Explore 43 results rather well, as it should if the discontinuities are representative of directional discontinuities.

The number of discontinuities per day is shown as a function of time in Figure 4. The rate of occurrence varies from 5/day to 45/day. These are minimum rates of occurrence, since we did not select all discontinuities. The important point demonstrated by Figure 4 is that we were observing discontinuities under a variety of interplanetary conditions: there were two kinds of shock flows (Ogilvie and Burlaga, 1974), at least three fast streams with well-defined interfaces (Burlaga, 1974), and 'Alfvénic fluctuations (Burlaga and Turner, 1976). The quantity ρ in Figure 4 is the correlation coefficient between the fluctuations in the speed and the radial component of the magnetic field. A value of $\rho > 0.6$ is taken as an indication of the presence of 'Alfvénic fluctuations, as discussed by Burlaga and Turner (1976). It is interesting to note that the discontinuities were most numerous (45) on the day (April 6) that 'Alfvénic fluctuations were most prominent.

3. Nature of the Discontinuities

The "discontinuities" that we have been discussing are not truly discontinuous, of course; they only appear to be so at low time resolution, or when the field is averaged over 30s or so. In general, there is a current sheet (boundary layer) in which the magnetic field direction changes continuously from one side of the 'discontinuity' to the other, as illustrated in Figure 5. If the "discontinuity" is tangential, all of the magnetic field vectors in the current sheet are parallel to the surface of the discontinuity, as drawn in Figure 5. If the "discontinuity" is rotational, then one component changes as in Figure 5, and there is another component which is constant and normal to the plane of the discontinuity. Thus, in principal, one can distinguish between a TD and an RD by analyzing the structure of the current sheet.

Sonnerup and Cahill (1967) introduced a technique for analyzing the structure of a current sheet; this is illustrated in Figure 6. Basically, the procedure is as follows: 1) determine the average of the magnetic field vectors in the current sheet, $< \underset{\sim}{B}_i >$, 2) for each vector $\underset{\sim}{B}_i$ in the current sheet, compute the difference $\Delta B_i \equiv \underset{\sim}{B}_i - < \underset{\sim}{B}_i >$, 3) find the plane which best fits the set of vectors $\Delta \underset{\sim}{B}_i$ (the minimum variance plane), and 4) determine the average component of $\underset{\sim}{B}_i$ normal to that plane. For a TD, the ΔB_i are all parallel to the surface of the discontinuity, since the $\underset{\sim}{B}_i$ themselves are parallel to that surface. Thus, there is no component of $\underset{\sim}{B}$ normal to the minimum variance surface of $\Delta \underset{\sim}{B}_i$ for a TD, as illustrated on the right side of Figure 6. For an RD, the vectors $\underset{\sim}{B}_i$ rotate on the surface of a cone, as shown on the left of Figure 6, and the surface of the discontinuity is the base of the cone. In this case, there is a

non-zero component of $\underset{\sim}{B}_i$ normal to the base of the cone (B_{ni}) and the other component of $\underset{\sim}{B}_i$ rotates parallel to this surface. For a RD, one eliminates B_{ni} by taking the difference $\Delta\underset{\sim}{B}_i = \underset{\sim}{B}_i - \langle \underset{\sim}{B}_i \rangle$, and the minimum variance surface of $\Delta\underset{\sim}{B}_i$ is the surface of the discontinuity. For a RD, one should find that $B_n \equiv \langle |B_{ni}| \rangle \equiv \frac{1}{N} \Sigma |B_i \cdot \hat{n}|$, is non-zero, (where N is the number of vectors in the current sheet and $\hat{n}$ is the normal to the minimum variance plane of the $\Delta\underset{\sim}{B}_i$).

In principal, the Sonnerup-Cahill technique determines the surface of the discontinuity and one can distinguish between a RD and a TD by determining whether or not there is an average component of $\underset{\sim}{B}$ normal to that surface. In practice, the technique can give misleading results if not used judiciously, since it can be very sensitive to experimental errors. The problem arises because the minimum variance plane and its normal can be determined only if the experimental errors in $\Delta\underset{\sim}{B}_i$ are small enough that the $\Delta\underset{\sim}{B}_i$ lie close to the plane.

The digitization error in the Explorer 43 magnetic field measurements is $\approx \pm 0.06\gamma$, and the RMS sensor noise in each component is 0.03γ - 0.05γ. Thus, the uncertainty in determining each component of the field is $\approx 0.07\gamma$. Now consider the size of the quantities to be measured, viz. $\Delta\vec{\underset{\sim}{B}}_i$. (See the base of the cone in Figure 6.) Suppose, for the purpose of illustration, that $B_n = 2\gamma$, $B_1 = B_2 = 5\gamma$, and $\omega = 30^\circ$. The length of the chord AB in Figure 6 is then 1.3γ. The component of $\Delta\underset{\sim}{B}_i$ in the direction along the arc of the circle ($\hat{t}$) is on the order of 0.65γ, which is small but well above the experimental errors. On the other hand, the component of $\Delta\underset{\sim}{B}_i$ along the radius of the circle in Figure 6 (ΔB_ρ) is less than ≈ 0.18, which is comparable to the experimental errors. Since the

magnitude of ΔB_ρ is comparable to the experimental errors in the $\hat{\rho}$ and $\hat{n}$ directions, the vectors $\Delta \underset{\sim}{B}_i$ will scatter appreciable about the $(\hat{\rho}, \hat{t})$ plane. Thus, the plane and its normal cannot accurately be determined in this case, and one might obtain a large B_n for a TD simply because the normal is wrong.

A more thorough error analysis by Behannon and Lepping (1976) (based on simulations of current sheets) showed that when $\omega \geq 60^\circ$, the uncertainties in B_n are $\leq 0.5\gamma$. For ω close to but greater than 30°, the uncertainties in B_n are $\leq 2\gamma$. For $\omega < 30^\circ$, the error in B_n can be very large and the Sonnerup-Cahill method cannot be used. Similar conclusions are obtained using the error analysis of Sonnerup (1971).

We selected the Explorer 43 discontinuities with $\omega > 30^\circ$ (there were 192 of them), and we applied Sonnerup's technique to each of the current sheets. Typically, there were 100 values of $\Delta \underset{\sim}{B}_i$ in each current sheet. In most cases, the surface of the discontinuity was satisfactorily determined. This is shown by Figure 7, which gives the distribution of λ_2/λ_3, the ratio of the intermediate to minimum eigenvalue. The most probable value of λ_2/λ_3 is $\simeq 3$, and the average is higher, 6.5, because the distribution is highly skewed.

The distribution of the average normal component, $B_n \equiv < |B_z| >$, is shown in Figure 8. There is a strong peak at $B_n = 0$, consistent with a population of TD's. The dashed curve, $54.1 \exp (- < |B_z| >/1.25)^2$, is a gaussian fit to the population near $< |B_z| > = 0$. This gives a $\sigma = 0.9\gamma$ for the variance, which is on the order of the errors derived from simulations of TD's by Behannon and Lepping (1976). We conclude that the events with $B_n < 2\gamma$ (or 1.5γ, depending on the confidence level that one

chooses) are consistent with being tangential discontinuities. Most of the events with $B_n > 3\gamma$ are probably RD's, since 3γ is far outside the experimental errors in most cases. Indeed, there is a peak in the distribution of B_n between 3.5γ and 4γ, which might be a characteristic of a population of RD's. The number of events with $B_n > 3\gamma$ is 43, and the number of events with $B_n < 2\gamma$ is 122. If our sample of discontinuities (which probably contains one-half to one-third of all discontinuities with $\omega > 30^\circ$) is representative, then the ratio of TD's to RD's defined in this way is 2.8. In other words, those results suggest that the ratio of TD's to RD's was typically 2.8 to 1 in the interval that we are considering.

The distribution of the normals of TD's has been discussed in several papers (see the reviews by Burlaga (1972) and Siscoe (1974), and the papers by Siscoe et al. (1968), Burlaga (1969), Smith (1973a), Turner (1973), and Turner and Siscoe (1971)). The general result is that the normals of TD's tend to be perpendicular to the spiral average magnetic field direction and close to but somewhat out of the ecliptic plane, while the normals of RD's are more randomly scattered. Figure 9 gives the distribution of normals for TD's and RD's in our data set. For this purpose, we identify those discontinuities with $B_n < 2\gamma$ as TD's and those with $B_n > 3\gamma$ as RD's. One sees that the distributions show the same general patterns that were suggested by the earlier work.

4. Discontinuities in the presence of 'Alfvénic Fluctuations'

It has been suggested that discontinuities are predominately rotational when there is a high correlation between $\delta\underset{\sim}{V}$ and $\delta\underset{\sim}{B}$, particularly when the speed is high and decreasing in a stream. We now consider whether or not this is in fact the case.

Let ρ be the correlation coefficient between the radial component of $\underset{\sim}{B}$ and V during an hour interval, as discussed by Burlaga and Turner (1976). Considering the experimental uncertainties, $\rho > 0.6$ is also consistent with $\rho = 1$ as required for 'Alfvénic fluctuations' (Burlaga and Turner, 1976), so we shall take $\rho > 0.6$ as an indication of Alfvénic fluctuations. A similar definition was used by Belcher and Davis (1971), Belcher and Solodyna (1975), and Martin et al. (1973).

The distribution of $< |B_z| >$ for discontinuities that occurred during hourly intervals in which $\rho > 0.6$, (i.e., for discontinuities among Alfvénic fluctuations) is shown in Figure 8. More than half of the discontinuities that we chose between March 15 and April 9 occurred under this condition (109 among 192). The distribution of $< |B_z| >$ for these discontinuities is very much like that for all of the events. In particular, the most probable value is zero, consistent with TD's, and there were 88 (81%) with $< |B_z| > < 2\gamma$. In other words, our results are consistent with TD's being predominate even in the presence of Alfvénic fluctuations.

Now let us consider a 24-hr. interval during which Alfvénic fluctuations ($\rho > 0.6$) were present throughout the day, viz. April 6, 1971. At this time, the spacecraft was in a well-defined stream; the speed was high and decreasing, as shown in Figure 10. The speed and radial

magnetic field profiles in Figure 10 are very much like those in Figure 1 of Belcher and Davis (1971) and in Figure 1 of Belcher and Solodyna (1975); those authors interpreted the variations as Alfvénic fluctuations. The Alfvénic nature of the fluctuations in Figure 10 is indicated by the high correlation between V and B_x ($\rho > 0.6$) and by the relatively small fluctuations in $|\underset{\sim}{B}|$ and in the density, n. We selected 45 discontinuities on this day, and we found that $\omega > 30^\circ$ for 37 of them.

The panel on the left of Figure 11 shows an example of a TD that was observed among the Alfvénic fluctuations on April 6. The components are shown in the minimum variance system: $\hat{z}$ is the minimum variance direction, $\hat{y}$ is normal to $\hat{z}$ and in the plane containing the average field and $\hat{z}$, and $\hat{x}$ completes the right-hand coordinate system. For this event, $\omega = 91.8^\circ$ and the ratio of the intermediate to minimum eigenvalue obtained using Sonnerup's method is $\lambda_2/\lambda_3 = 6.5$, so the minimum variance plane was well determined. The average component of normal to this plane is $B_n = 0.16\gamma$, so the discontinuity is clearly a TD. This boundary layer happens to be rather smooth. A less regular boundary layer, which occurred at 1450 on April 6, is shown on the right of Figure 11. In this case $\omega = 97.6^\circ$, $(\lambda_2/\lambda_3) = 17.1$, indicating a well-defined minimum variance plane, and $B_n = 0.58\gamma$, which is consistent with zero. Thus, this too is apparently a TD among Alfvénic fluctuations. Table 1 summarizes the properties of 12 boundary layers with $B_n < 1\gamma$ that occurred on April 6 (note that $B_n < 0.5\gamma$ for half of these). They are all consistent with being TD's, and all occur in the presence of Alfvénic fluctuations. Their relation to these fluctuations is shown by the vertical lines in Figure 10.

Examples of RD's on April 6, are shown on Figure 12. For the event at 0357 UT, shown on the left of Figure 12, the change in angle was small ($\omega = 37^\circ$), but the minimum variance plane was well determined ($\lambda_2/\lambda_3 = 10.6$). The component of $\underset{\sim}{B}$ normal to this plane was 4.4γ in an average field of 5γ. The event of 0239 UT, shown on the right of Figure 12, was somewhat broader, the angular change was larger ($\omega = 70.3^\circ$), and the minimum variance plane was less well defined ($\lambda_2/\lambda_3 = 2.2$), but again we find a large normal, $B_n = 4.0\gamma$ in a 5γ field. Thus, there is little doubt that RD's can also occur among Alfvénic fluctuations.

The general character of the discontinuities with $\omega > 30^\circ$ on April 6, is summarized in Figure 13, which shows the distribution of $B_n \equiv < |B_z| >$ for this day. There were 37 discontinuities, 1.5/hr. There is a peak in the B_n distribution at $B_n = 0$, consistent with the presence of TD's. For 16 events (43%), $B_n < 2\gamma$; these events are probably TD's since the uncertainties are approximately 1 or 2γ. In addition, there is a second peak in the B_n distribution between 3.5γ and 4γ. For 17 events (46%), $B_n > 3\gamma$, and these events are probably RD's. Thus, during this Alfvénic period, the B_n distribution is atypical (compared to that in Figure 8), being bimodal with roughly equal numbers of TD's and RD's.

We conclude that: 1) TD's can coexist with Alfvénic fluctuations, 2) RD's are not necessarily predominant in the presence of Alfvénic fluctuations, but 3), RD's occur preferentially with Alfvénic fluctuations in high-speed streams. The association of RD's with Alfvénic fluctuations is not surprising since RD's themselves satisfy the conditions for an Alfvénic wave.

5. Thickness of "Laminar Boundary Layers"

Sestero (1964) and Lemaire and Burlaga (1976) developed a theory for the structure of "laminar" boundary layers, i.e., those in which the magnetic field varies smoothly in the current sheet. Their results predict that the thickness of such a current sheet should be on the order of a few to several proton Larmor radii, depending on the details of the distribution function in the current sheet and on the conditions on both sides of the sheet. To compare this theory with observations, we selected the subset of boundary layers for which a) the magnetic field changed very smoothly in the layer, b) there was a well-defined beginning and end of the layer, and c) plasma data are available.

The boundary layers are convected with the solar wind past the spacecraft. Let the interval during which a layer moves past the spacecraft be denoted by T. The thickness (ξ) of a boundary layer is related to T, the solar wind speed (V), and the radial component of the unit vector normal to the discontinuity surface ($|n_r|$) by the formula

$$\xi = V\,|n_r|\,T. \qquad (2)$$

In order to accurately determine n_r using the minimum variance method, it is necessary to again restrict our attention to discontinuities with $\omega > 30^\circ$.

The "thickness" distributions for TD's (defined by $B_n < 2\gamma$) are shown in Figure 14. The most probable duration is 2.5 ± 0.5 sec, and the average is 4.7 sec. Seventy percent of the durations were less than 10 sec, and 98% were less than 15 sec. The shortest duration was 0.6 sec. The thickness ranged from 158 km to 8,000 km; in terms of proton gyroradii, R_L, the thickness ranged from 1.5 R_L to 82 R_L. The average thickness of the TD's was 1,300 km and 12 R_L.

The "thickness" distributions for RD's, (defined by $B_n > 3\gamma$) is shown in Figure 15. They are similar to the distributions for TD's. The most probable duration for the RD's is 5 ± 1 sec. The average is 5.4 sec, and the range is from 1.1 sec to 14.7 sec. The average thickness is 1,200 km (13 R_L), and the range is from 250 km (2.2 R_L) to 2,500 km (43 R_L).

6. Summary

We have examined the nature and characteristics of discontinuities in the interplanetary magnetic field during the period March 18, 1971 to April 9, 1971. This period contained a variety of interplanetary conditions--simple and compound streams, shock flows, irregular speed variations, stream interfaces, shock fronts, and 'Alfvénic fluctuations'. The discontinuities, which we identified visually in plots of 1.28 sec averages of the magnetic field data, occurred under all of these conditions. The rate ranged from 5/day to 45/day, with an average of 0.7/hr. This is a minimum rate, for we did not attempt to include all discontinuities present. Discontinuities with a small change in the magnetic field direction were discarded, giving a rate of 0.5/hr for the discontinuities that were analyzed in detail. The total rate of discontinuities may be two or three times that which we observed, but our sample is probably representative of discontinuities with $\omega > 30^{\circ}$; in any case, it is an order of magnitude larger than samples which have been used in the past to study the nature and internal structure of discontinuities.

The Explorer 43 observations were quite accurate, and the sampling rates were such that typically 100 vector measurements were made in the boundary layer associated with a discontinuity. Thus, we were able in most cases to apply Sonnerup's minimum variance method to determine the orientation of the surface associated with a discontinuity and the component of $\underset{\sim}{B}$ normal to this surface (B_n). Our analysis was restricted to discontinuities across which the change in the direction of $\underset{\sim}{B}$ was greater than 30°, in order to eliminate events for which the orientation of the surface was not accurately determined. The distribution of B_n

is peaked at $B_n = 0$ and the distribution near zero falls off as a gaussian with a variance of 1γ; we interpret the events with $B_n < 2\gamma$ as tangential discontinuities, since 2γ is consistent with zero within the errors. In addition, there is an extended tail up to $B_n = 10\gamma$ and a possible peak between 3.5γ and 4γ; we interpret the events with $B_n > 3\gamma$ as rotational discontinuities. The ratio of TD's to RD's obtained in this way for the period March 18, 1971 to April 9, 1971, is 2.8 to 1.

We have examined the issue of whether or not TD's can occur in the presence of Alfvénic fluctuations and the question of relative abundance of RD's and TD's in regions of high and decreasing speeds where Alfvénic fluctuations are most pronounced. We found that TD's do indeed occur in such periods. In fact, we showed that during one interval lasting 24 hours TD's occurred at the rate of at least 0.5/hr. On the other hand, we also found that the B_n distribution was bimodal in this interval, with roughly equal numbers of TD's and RD's, suggesting that RD's preferentially occur in such intervals.

The structure of the boundary layer was clearly resolved in every case that we considered. Considering the subset of very regular boundary layers with well-defined beginning and end, we found that the average thickness of TD's was 13,000 km (12 R_L), and the average thickness of RD's was 12,000 km (13 R_L). The Larmor radius was somewhat larger on average in the intervals containing TD's than in the intervals containing RD's.

Acknowledgments

The results of this paper are based on the accurate, high-resolution magnetic field data from the GSFC magnetometer on Explorer 43; we are indebted to Drs. Ness and Fairfield for allowing us to use these data for our investigation. The plasma data were obtained from the GSFC plasma experiment on Explorer 43, and we are likewise indebted to Dr. Ogilvie. We acknowledge important discussions with Drs. Behannon, Belcher, and Lepping. Mrs. P. Harris assisted in the programming. One of us (J. L.) was supported by the NAS/NRC, during part of this work.

Figure Captions

Figure 1 An example of a discontinuity. In this case, the direction of the magnetic field charged by 75°, somewhat larger than average (60°). This satisfies the definition for a directional discontinuity introduced by Burlaga (1969).

Figure 2 Examples of other discontinuities that were selected. The events shown here do not satisfy the definition of a directional discontinuity, because the change in direction (ω) is small and/or the discontinuities are too close together. They were included in the initial selection because the changes appear to be nearly discontinuous.

Figure 3 This is the distribution of ω, the change in direction of the magnetic field across the discontinuities that were selected. For 31% of the discontinuities, $\omega < 30^{\circ}$. The solid curve for $\omega > 30^{\circ}$ is $N = N_o \exp (-\omega/75^{\circ})^2$, which is the same function that Burlaga (1969) found for the ω-distribution of directional discontinuities in Pioneer 6 data.

Figure 4 This shows 1) the flow configuration in the period that is considered in this paper, 2) the correlation (ρ) between speed and the radial component of the magnetic field, which indicates the presence of "Alfvénic' fluctuations when it is large (> 0.6), and 3) the number of discontinuities per day as a function of time. The main point is that the discontinuities that we selected are found under a wide variety of interplanetary conditions.

Figure 5 The transition between the two sides of a 'discontinuity' is actually a continuous one, and is called a boundary layer or current sheet. For a tangential discontinuity, the magnetic field vector rotates in the boundary layer from one state to another, always remaining parallel to the surface of the 'discontinuity', as shown here. For an RD, one component of $\underset{\sim}{B}$ rotates as shown here, and in addition there is a component of $\underset{\sim}{B}$ perpendicular to the surface of the 'discontinuity'.

Figure 6 For an RD, the magnetic field rotates on the surface of a cone as shown at the left, while for a TD it rotates in a plane as shown on the right. The Sonnerup-Cahill method determines the plane which contains $\Delta\underset{\sim}{B}_i = \underset{\sim}{B}_i - \langle \underset{\sim}{B}_i \rangle$. For an RD there is a non-zero component of $\underset{\sim}{B}$ normal to this plane, while for a TD there is no component of $\underset{\sim}{B}$ normal to this plane. The determination of the plane containing $\Delta\underset{\sim}{B}_i$ is uncertain when ω is small, because some of the $\Delta\underset{\sim}{B}_i$ are too small to measure accurately in this case.

Figure 7 The distribution of the ratio of the intermediate eigenvalue (λ_2) to the minimum eigenvalue (λ_3) from the minimum variance analysis of the $\Delta\underset{\sim}{B}_i$. This quantity must be large if one is to accurately determine the minimum variance plane of $\Delta\underset{\sim}{B}_i$. One sees that it is large for most of the discontinuities with $\omega > 30^\circ$.

Figure 8 This shows the distribution of $< |B_z| >$, the component of $\underset{\sim}{B}$ normal to the minimum variance plane of $\Delta\underset{\sim}{B}_i$. Only discontinuities with $\omega > 30^\circ$ are considered, so that the minimum variance plane is well determined. The peak is at $< |B_z| > = 0$ and there is a population of events with $< |B_z| > < 2\gamma$, consistent with TD's. There is another population with $< |B_z| >> 3\gamma$ consistent with RD's. The ratio of TD's to RD's obtained in this way is 2.8 to 1. One obtains essentially the same distribution when only 'Alfvénic' ($\rho > 0.6$) periods are considered.

Figure 9 The distribution of the normals to the surfaces of TD's and RD's. Both tend to be above the ecliptic plane. The TD-normals tend to be normal to the spiral field; whereas, the RD-normals are more isotropically distributed.

Figure 10 An Alfvénic period. The fluctuations in V and B_x are highly correlated (the correlation coefficient ρ being greater than 0.6 throughout the day), and the density and magnetic field intensity are relatively constant, indicating Alfvénic fluctuations. Fourty-five discontinuities were observed during this day, as shown by the vertical lines in the top panel. Several of these were tangential discontinuities, as indicated by the vertical lines extending through all of the panels.

Figure 11 The structure of two TD's. In both cases, the magnetic field intensity is nearly constant, and the field vector rotates in a plane. The component normal to this plane

(B_z) is consistent with zero in both cases, indicating that the discontinuities are tangential.

Figure 12 The structure of two RD's. The magnetic field intensity is constant and the magnetic field rotates on a cone. The component $\underline{B}$ normal to the base of the cone is large in both cases, indicating that the discontinuities are rotational.

Figure 13 The distribution of $< |B_z| >$ for the discontinuities on April 6. It is bimodal and suggests equal numbers of TD's and RD's.

Figure 14 'Thickness' distributions for TD's.

Figure 15 'Thickness' distributions for RD's.

References

Behannon, K. and R. L. Lepping (private communication, 1976).

Belcher, J. W. and L. Davis, Jr., Large amplitude Alfvén waves in the interplanetary medium, J. Geophys. Res., 76, 3534, 1971.

Belcher, J. W. and C. V. Solodyna, Alfvén waves and directional discontinuities in the interplanetary medium, J. Geophys. Res., 80, 181, 1975.

Burlaga, L. F., Directional discontinuities in the interplanetary magnetic field, Solar Phys., 7, 54, 1969.

Burlaga, L. F., On the nature and origin of directional discontinuities, J. Geophys. Res., 76, 4360, 1971.

Burlaga, L. F., Microstructure of the interplanetary medium, The Solar Wind, ed. C. P. Sonett, P. J. Coleman, Jr., and J. M. Wilcox, NASA SP-308, 1972.

Burlaga, L. F., Interplanetary stream interfaces, J. Geophys. Res., 79, 3717, 1974.

Burlaga, L. F. and K. W. Ogilvie, Solar wind temperature and speed, J. Geophys. Res., 78, 2028, 1973.

Burlaga, L. F. and J. M. Turner, Alfvén waves in the solar wind, J. Geophys. Res., 81, 73, 1976.

Denskat, J. and L. F. Burlaga, Multi-spacecraft observations of microscale fluctuations in the solar wind, submitted to J. Geophys. Res., 1976.

Fairfield, D., Whistler waves observed upstream from collisionless shocks, J. Geophys. Res., 79, 1368, 1974.

Lemaire, J. and L. F. Burlaga, Diamagnetic boundary layers in the solar wind: A kinetic theory, to appear in Astrophysics and Space Sci., 1976.

Martin, R. N., J. W. Belcher, and A. J. Lazarus, Observations and analysis of abrupt changes in the interplanetary velocity and magnetic field, J. Geophys. Res., 78, 3653, 1973.

Ogilvie, K. W. and L. F. Burlaga, A discussion of interplanetary shock waves, with two examples, J. Geophys. Res., 79, 2324, 1974.

Sestero, A., Structure of plasma sheaths, Physics of Fluids, 7, 44, 1964.

Siscoe, G. L., Discontinuities in the solar wind in Solar Wind Three, p. 150, ed. C. T. Russell, published by Institute of Geophysics and Planetary Physics, University of California, Los Angeles, 1974.

Siscoe, G. L., L. Davis, Jr., P. J. Coleman, Jr., E. J. Smith, and D. C. Jones, Power spectra and discontinuities of the interplanetary magnetic field: Mariner 4, J. Geophys. Res., 73, 61, 1968.

Smith, E. J., Identification of interplanetary tangential and rotational discontinuities, J. Geophys. Res., 78, 2054, 1973a.

Smith, E. J., Observed properties of interplanetary rotational discontinuities, J. Geophys. Res., 78, 2088, 1973b.

Solodyna, C. V., J. W. Sari, and J. W. Belcher, Plasma-field characteristics of directional discontinuities in the interplanetary medium, submitted to J. Geophys. Res., 1976.

Sonnerup, B. U. Ö., Magnetopause structure during the magnetic storm of September 24, 1961, J. Geophys. Res., 76, 6717, 1971.

Sonnerup, B. U. Ö. and L. J. Cahill, Jr., Magnetopause structure and attitude from Explorer 12 observations, J. Geophys. Res., 72, 171, 1967.

Turner, J. M., On the relation between solar wind structure and solar wind rotational and tangential discontinuities, J. Geophys. Res., 78, 59, 1973.

Turner, J. M. and G. L. Siscoe, Orientations of rotational and tangential discontinuities in the solar wind, J. Geophys. Res., 76, 1816, 1971.

TABLE I

TD's on April 6, 1971

Time	$< B_z >$	ω^p	λ_2/λ_3
0408	- 0.19	30.4	2.0
0525	- 0.78	53.4	13.5
1004	0.32	78.9	4.3
1450	0.54	97.6	17.1
1621	0.16	91.8	6.5
1638	0.25	167.7	3.6
1714	0.34	35.3	7.8
1716	0.21	61.9	8.6
1827	0.62	30.0	1.9
1838	0.65	81.9	7.5
2022	0.85	106.0	6.4
2347	0.52	78.4	3.4

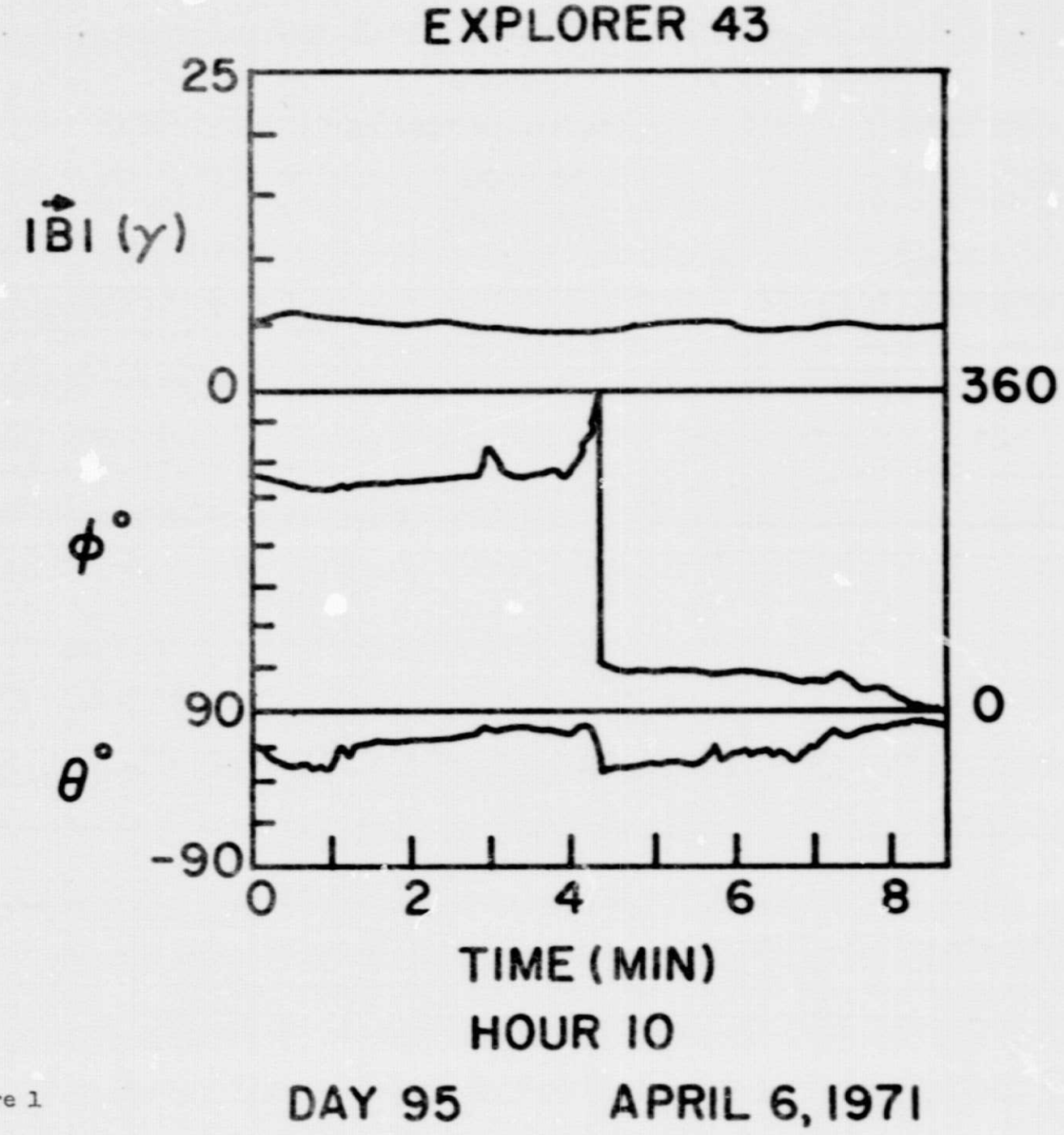
EXPLORER 43
25
|B| (γ)
0
360
φ°
90
0
θ°
-90
0
2
4
6
8
TIME (MIN)
HOUR 10
DAY 95
APRIL 6, 1971

Figure 1

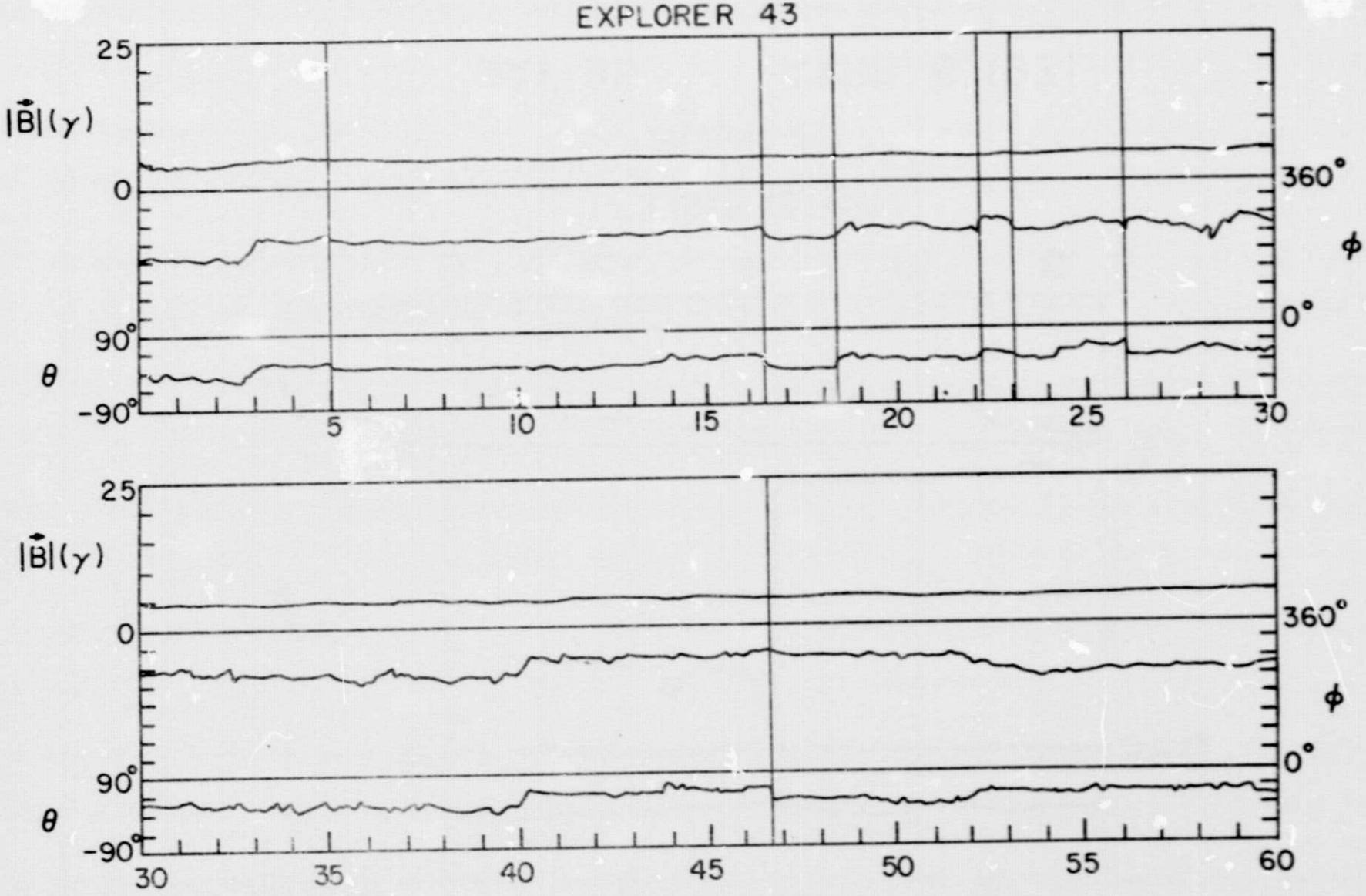
EXPLORER 43
25
|B|(γ)
0
90°
θ
-90°
360°
φ
0°
5
10
15
20
25
30
25
|B|(γ)
0
90°
θ
-90°
360°
φ
0°
30
35
40
45
50
55
60
TIME (MIN)
HOUR 5
DAY 95, APRIL 6, 1971

Figure 2

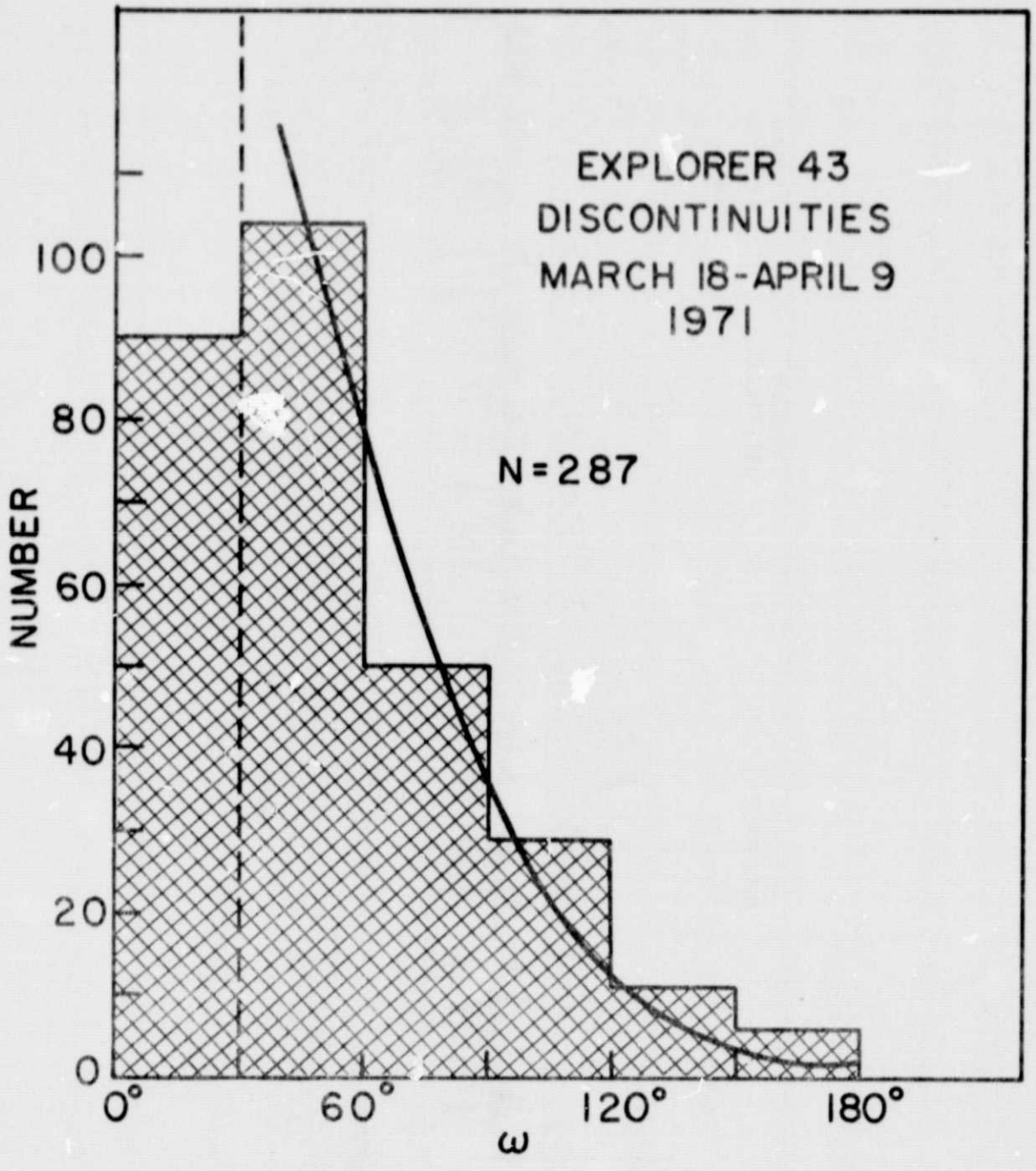
EXPLORER 43
DISCONTINUITIES
MARCH 18-APRIL 9
1971
N=287
NUMBER
100
80
60
40
20
0
0°
60°
120°
180°
ω

Figure 3

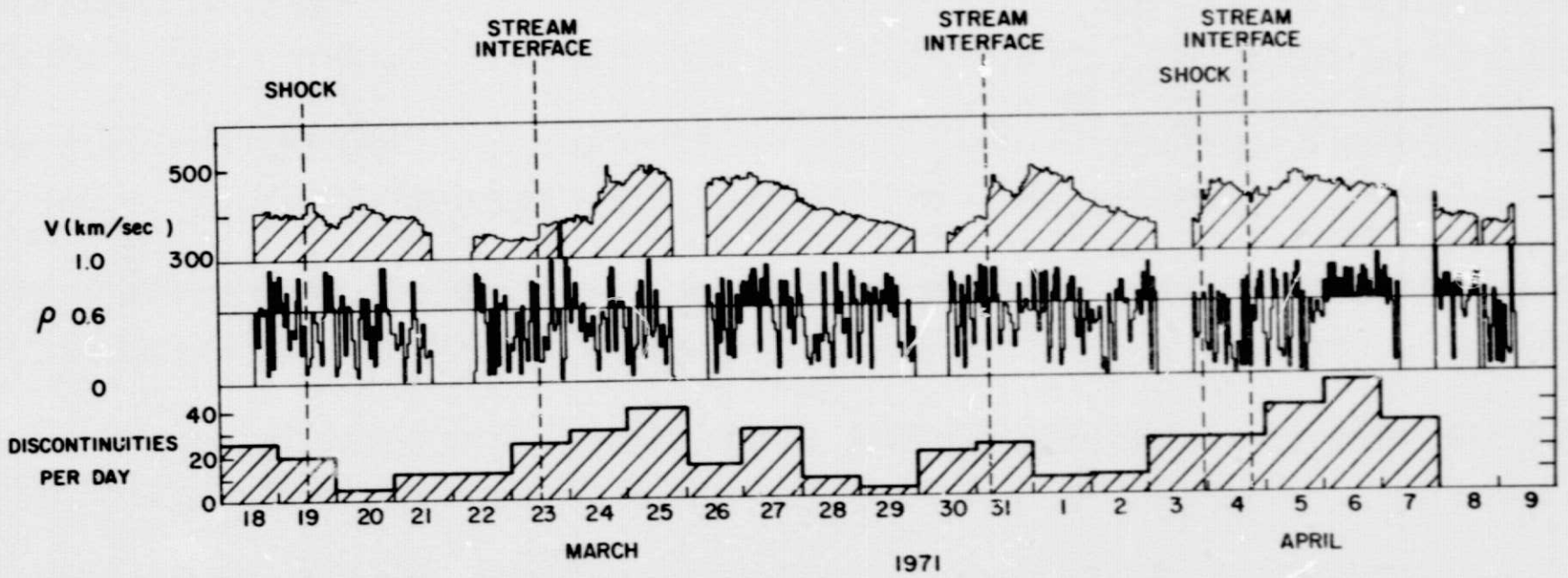
STREAM INTERFACE
STREAM INTERFACE
STREAM INTERFACE
SHOCK
SHOCK
V (km/sec)
500
300
1.0
ρ 0.6
0
DISCONTINUITIES PER DAY
40
20
0
18 19 20 21 22 23 24 25 26 27 28 29 30 31 1 2 3 4 5 6 7 8 9
MARCH
1971
APRIL

Figure 4

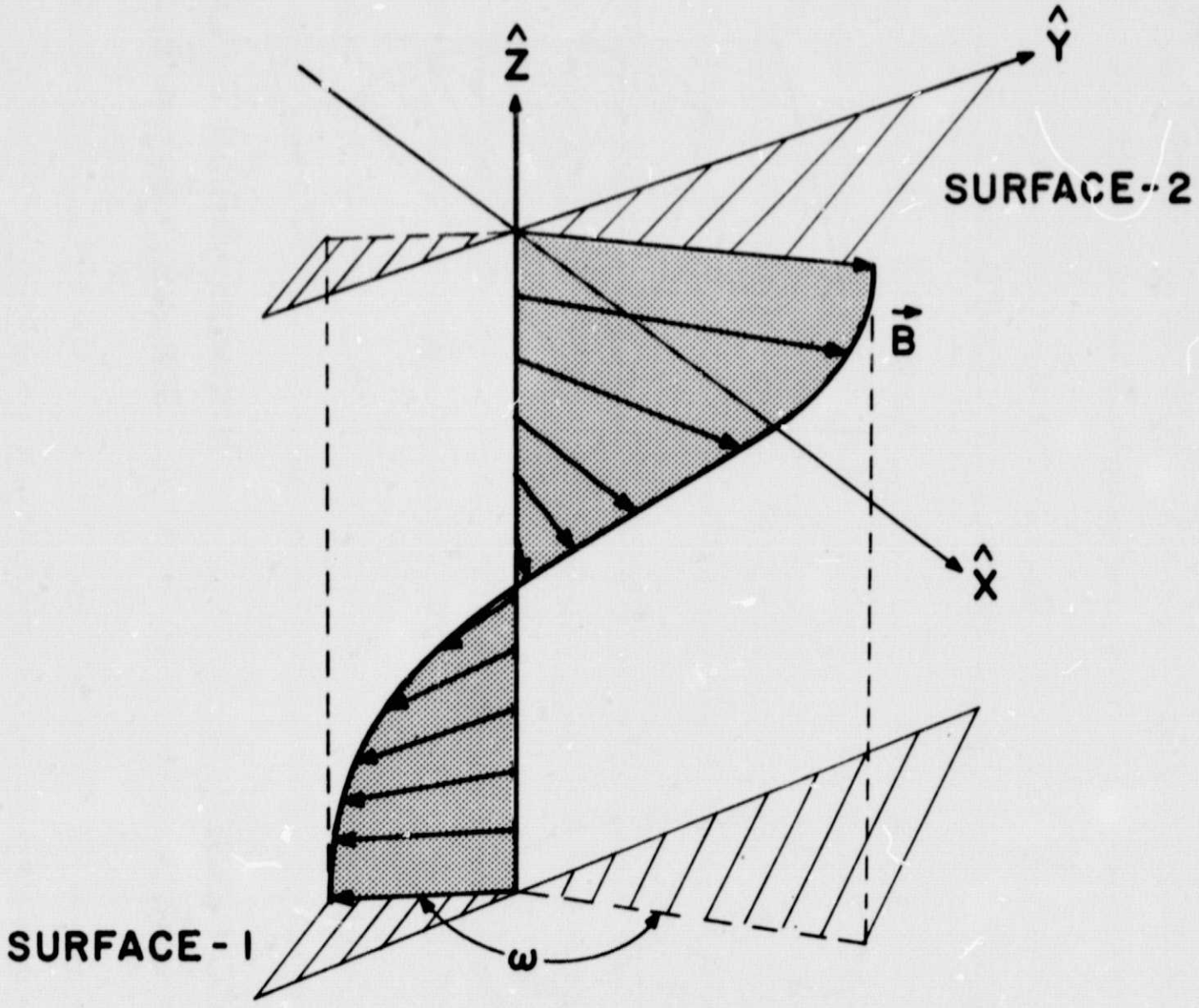

BOUNDARY LAYER

Figure 5

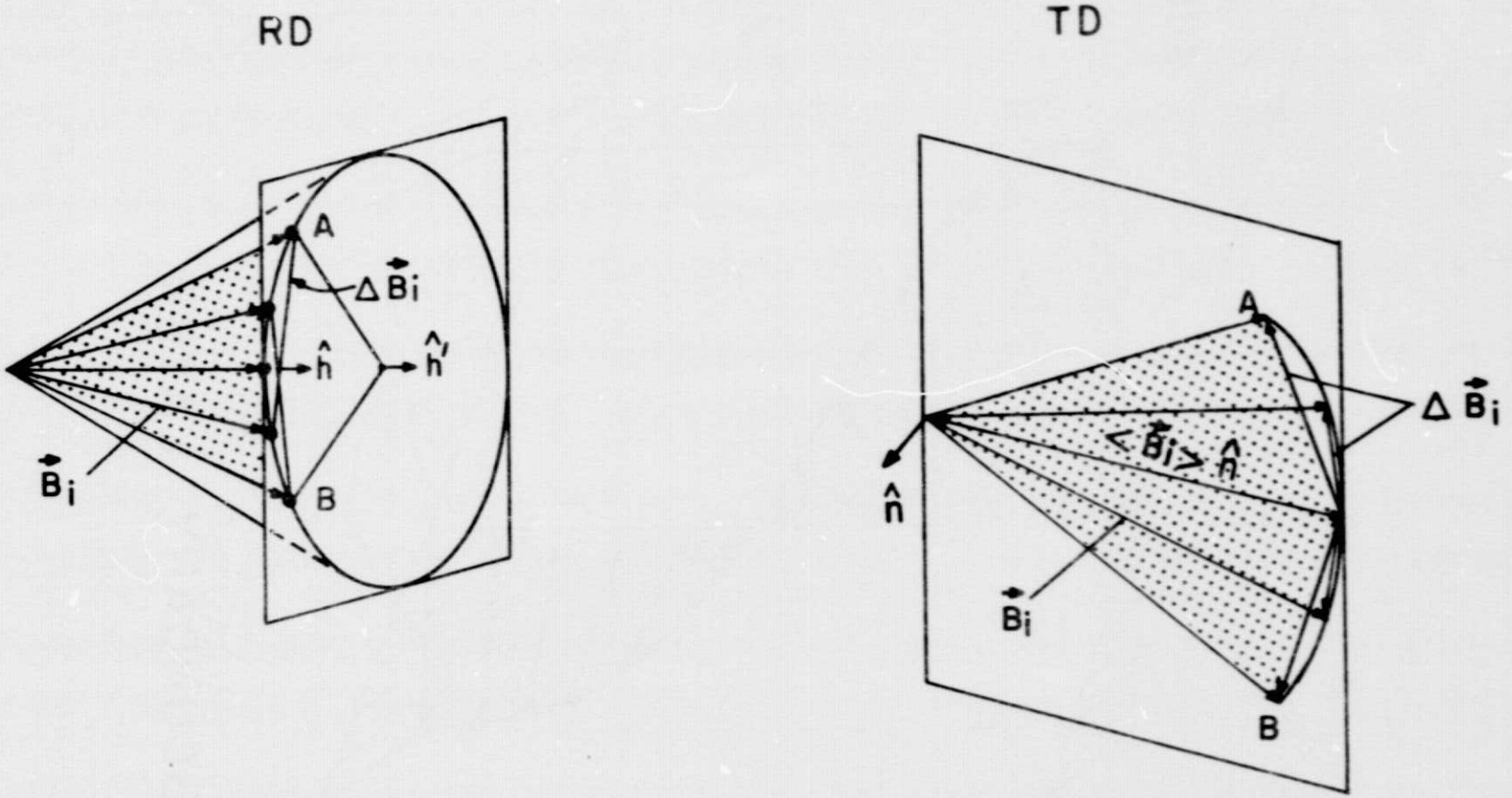
RD
TD
A
$\Delta \vec{B}_i$
$\hat{h}$
$\hat{h}'$
$\vec{B}_i$
B
$\hat{n}$
$\langle \vec{B}_i \rangle \hat{n}$
MINIMUM VARIANCE PLANE
FOR $\Delta \vec{B}_i = \vec{B}_i - \langle \vec{B}_i \rangle$
MINIMUM VARIANCE PLANE
FOR $\Delta \vec{B}_i = \vec{B}_i - \langle \vec{B}_i \rangle$

Figure 6

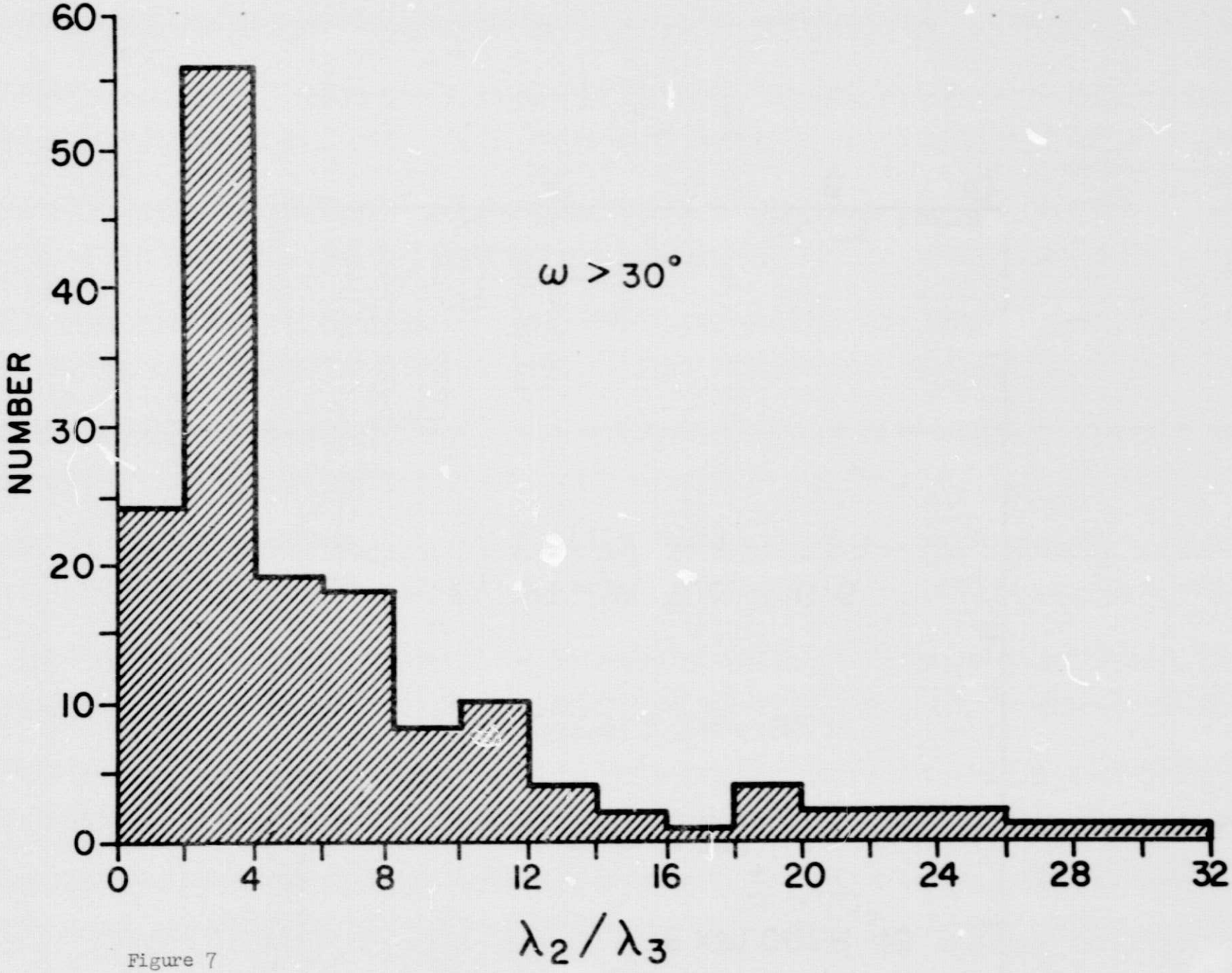

Figure 7

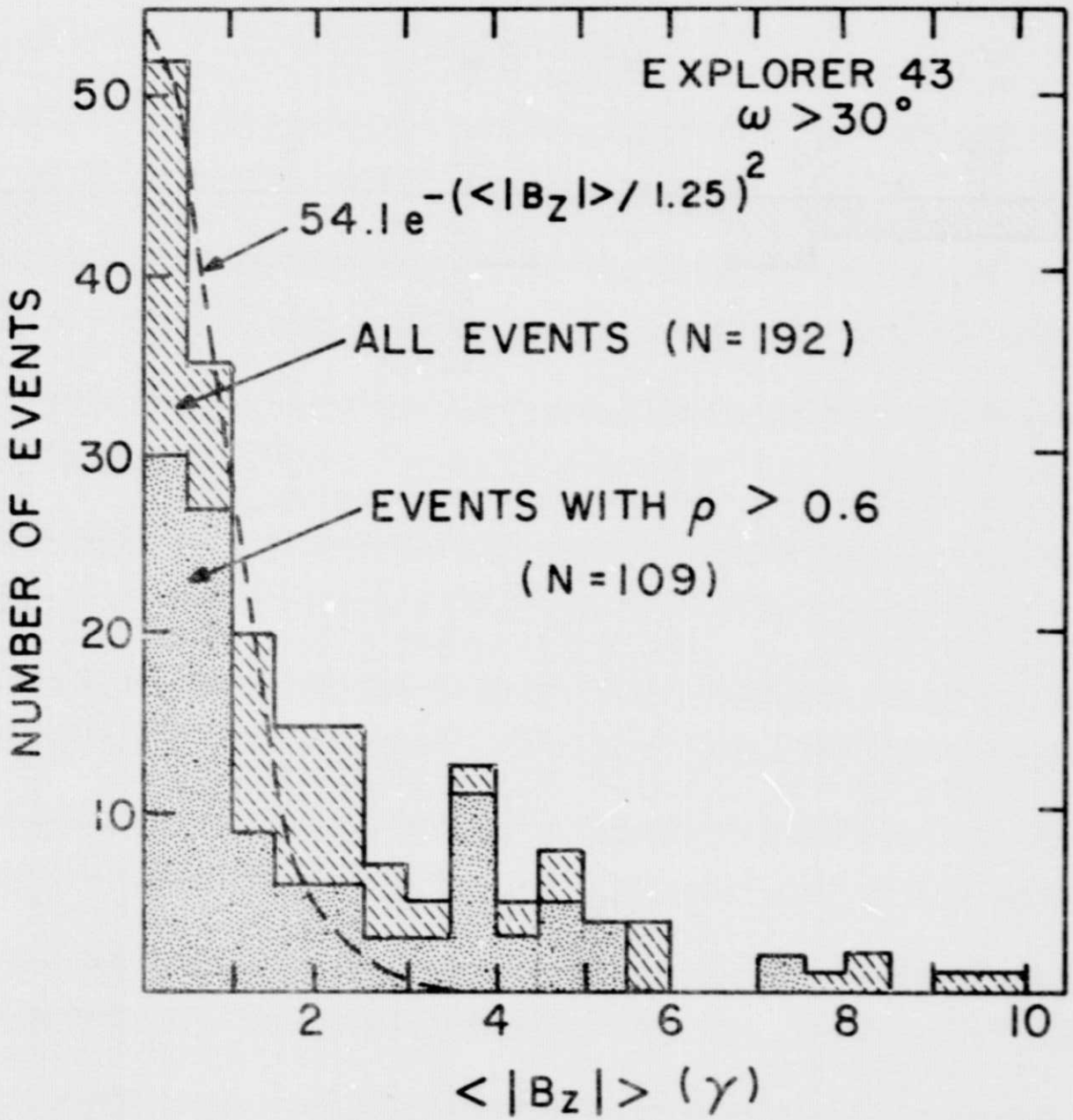
EXPLORER 43
ω >30°
54.1 e^-(<|Bz|>/ 1.25)^2
ALL EVENTS (N = 192)
EVENTS WITH ρ > 0.6
(N = 109)
NUMBER OF EVENTS
50
40
30
20
10
2
4
6
8
10
<|Bz|> (γ)

Figure 8

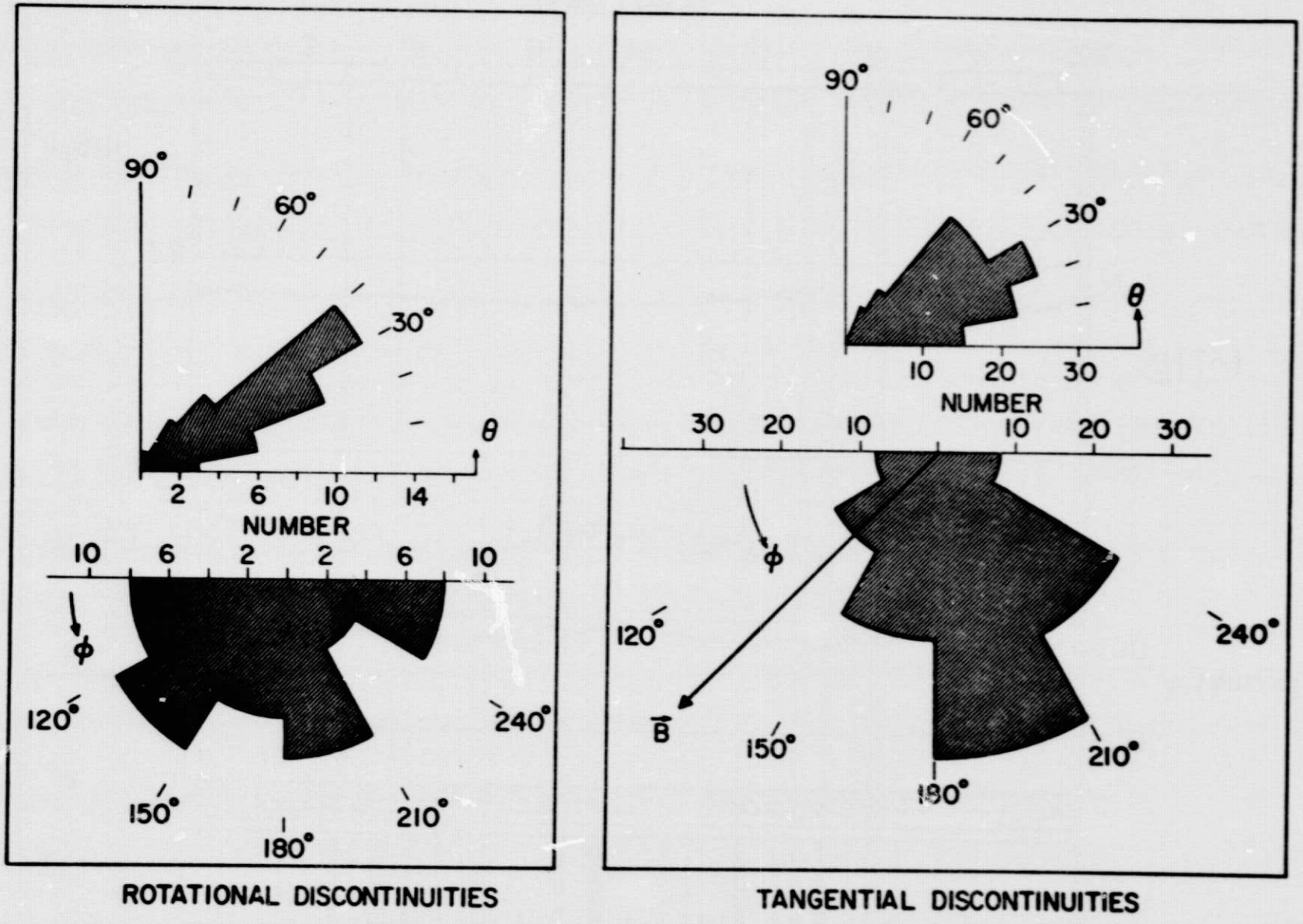
90°
60°
30°
θ
2
6
10
14
NUMBER
10
6
2
2
6
10
φ
120°
240°
150°
210°
180°
ROTATIONAL DISCONTINUITIES
90°
60°
30°
θ
10
20
30
NUMBER
30
20
10
10
20
30
φ
120°
240°
B
150°
210°
180°
TANGENTIAL DISCONTINUITIES

Figure 9

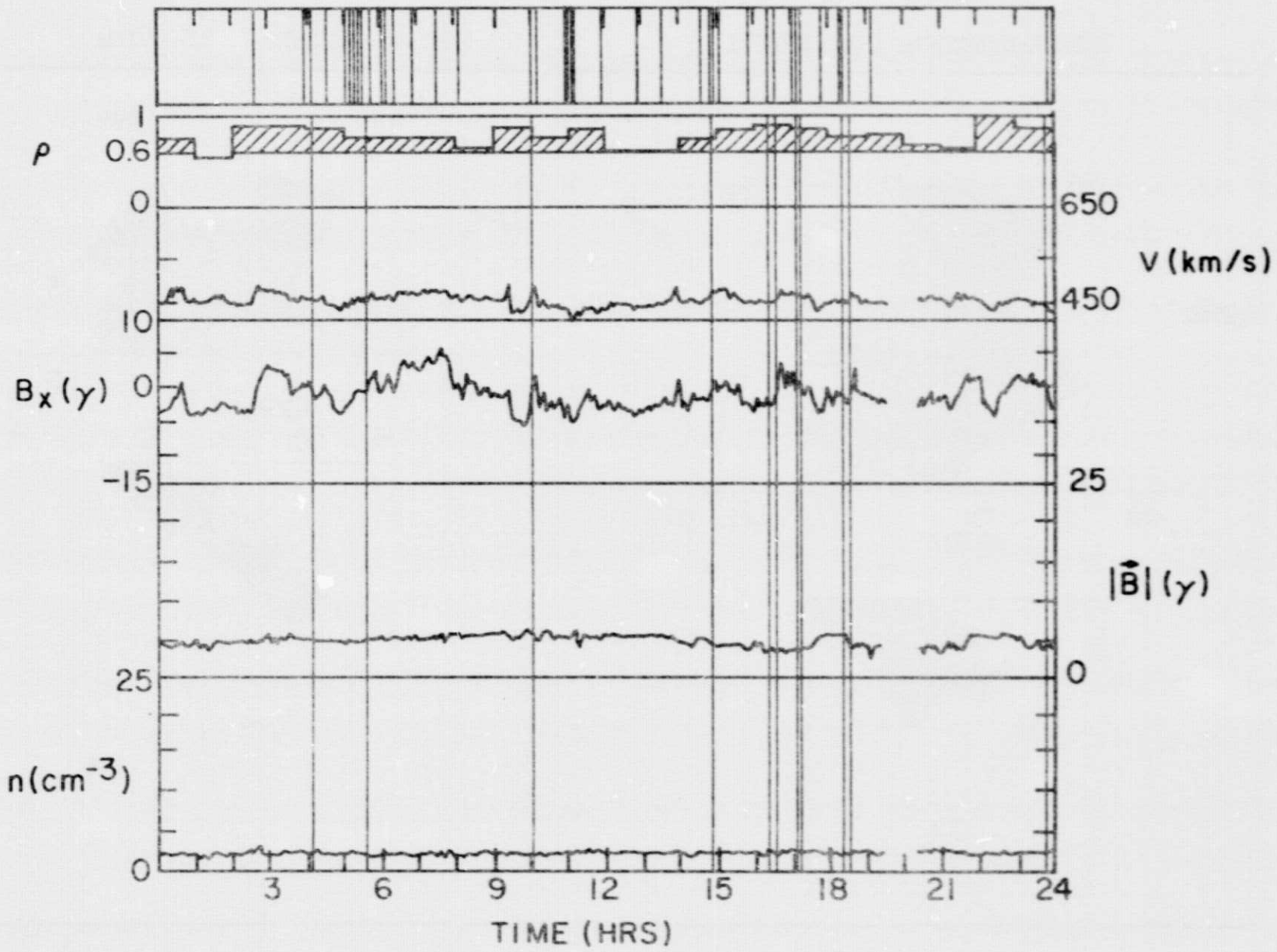
EXPLORER 43
ρ
1
0.6
0
650
V (km/s)
450
10
B_x (γ)
0
-15
25
|B| (γ)
0
25
n(cm^{-3})
0
3
6
9
12
15
18
21
24
TIME (HRS)
DAY 95, APRIL 6, 1971

Figure 10

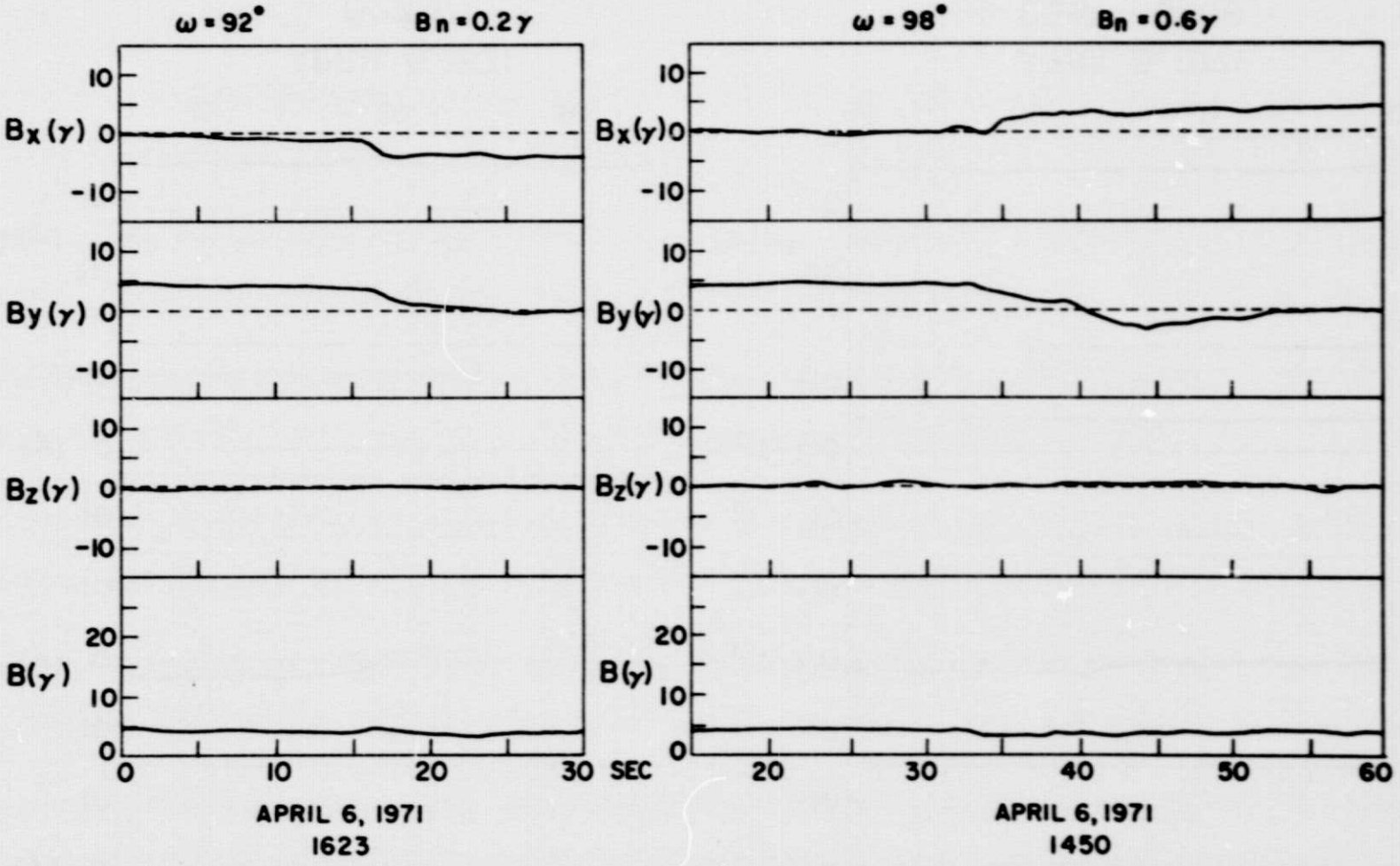
ω = 92°
Bn = 0.2γ
ω = 98°
Bn = 0.6γ
Bx (γ)
By (γ)
Bz (γ)
B(γ)
10
0
-10
20
0
10
20
30
SEC
40
50
60
APRIL 6, 1971
1623
APRIL 6, 1971
1450

Figure 11

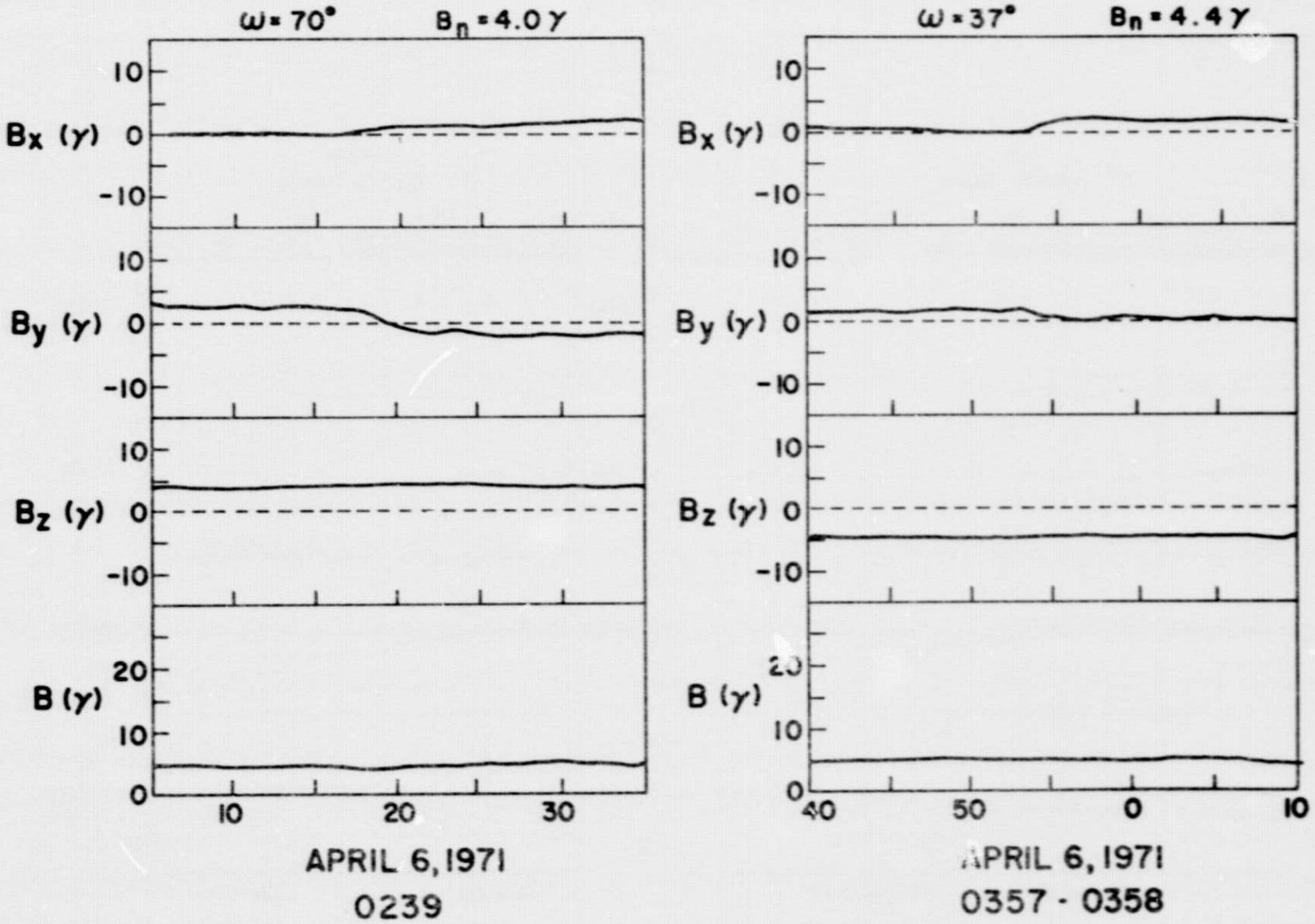
ω = 70°
Bn = 4.0 γ
Bx (γ)
By (γ)
Bz (γ)
B (γ)
10
0
-10
20
10
0
10
20
30
APRIL 6, 1971
0239
ω = 37°
Bn = 4.4 γ
40
50
0
10
APRIL 6, 1971
0357 - 0358

Figure 12

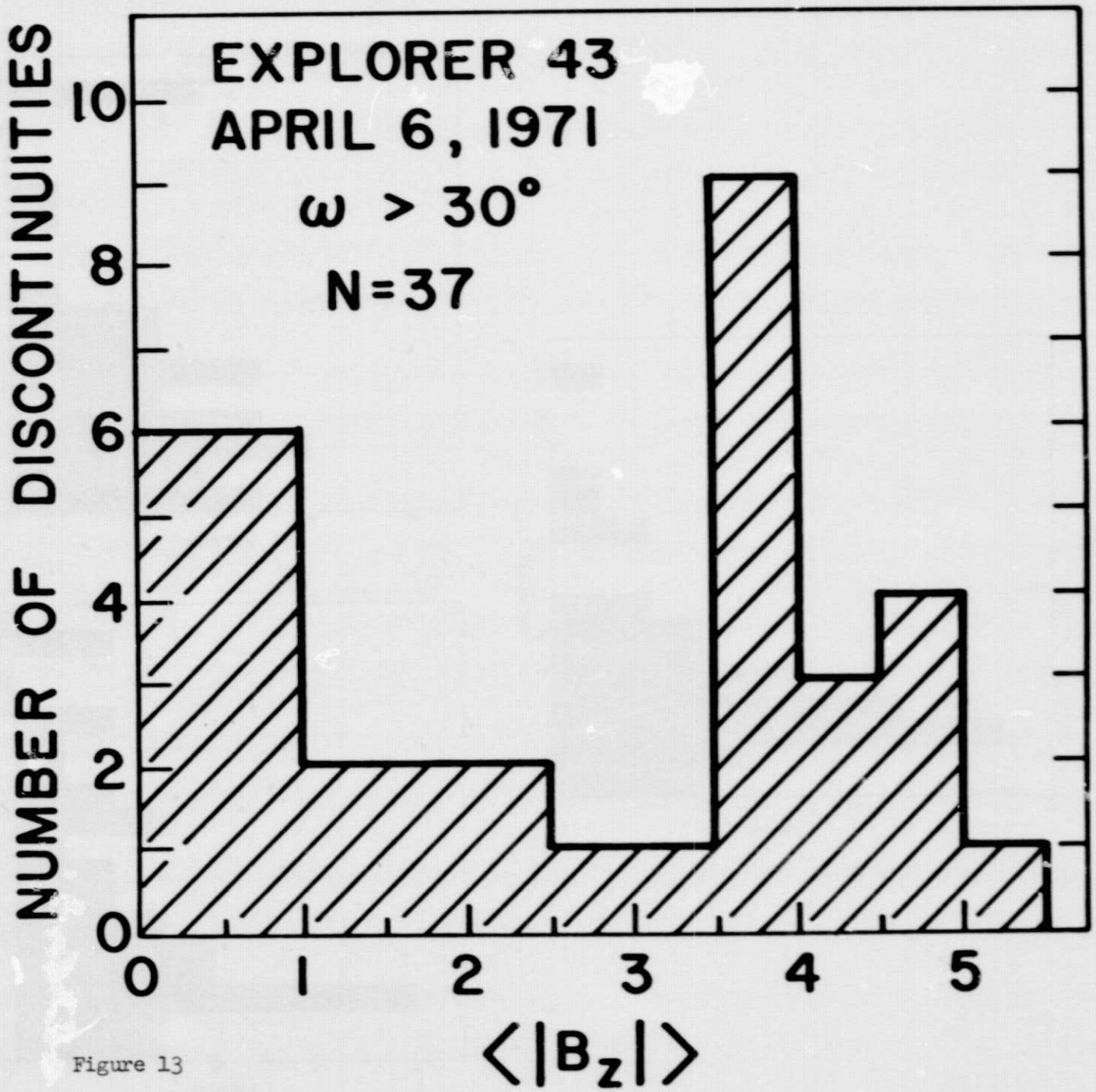
EXPLORER 43
APRIL 6, 1971
ω > 30°
N=37
NUMBER OF DISCONTINUITIES
0
2
4
6
8
10
0
1
2
3
4
5
⟨|Bz|⟩

Figure 13

TANGENTIAL
DISCONTINUITIES
EXPLORER 43
$\omega > 30^{\circ}$

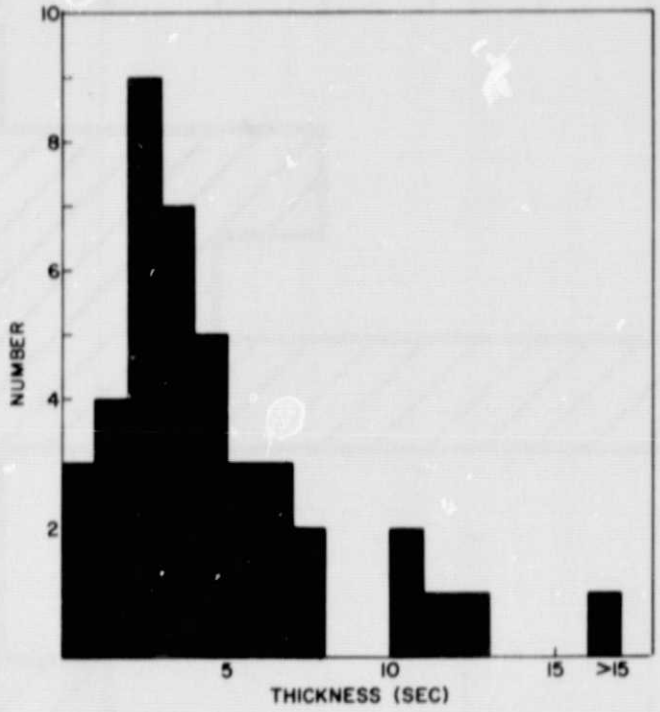

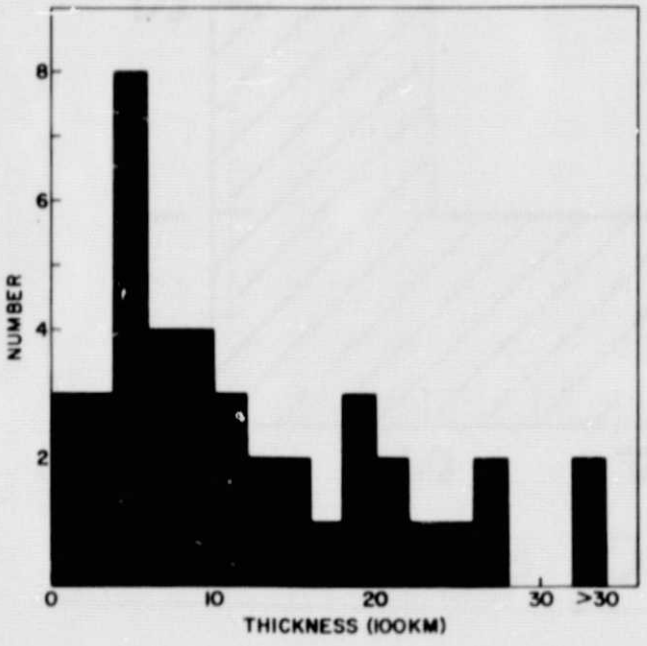

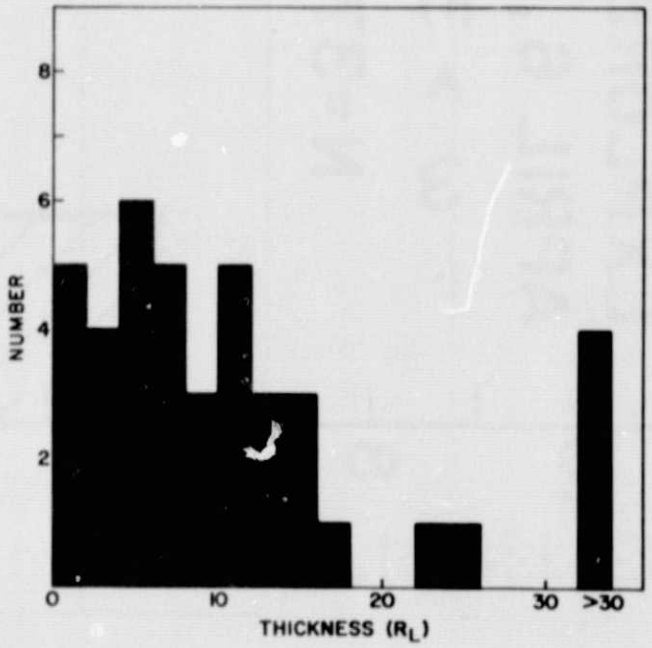

Figure 14

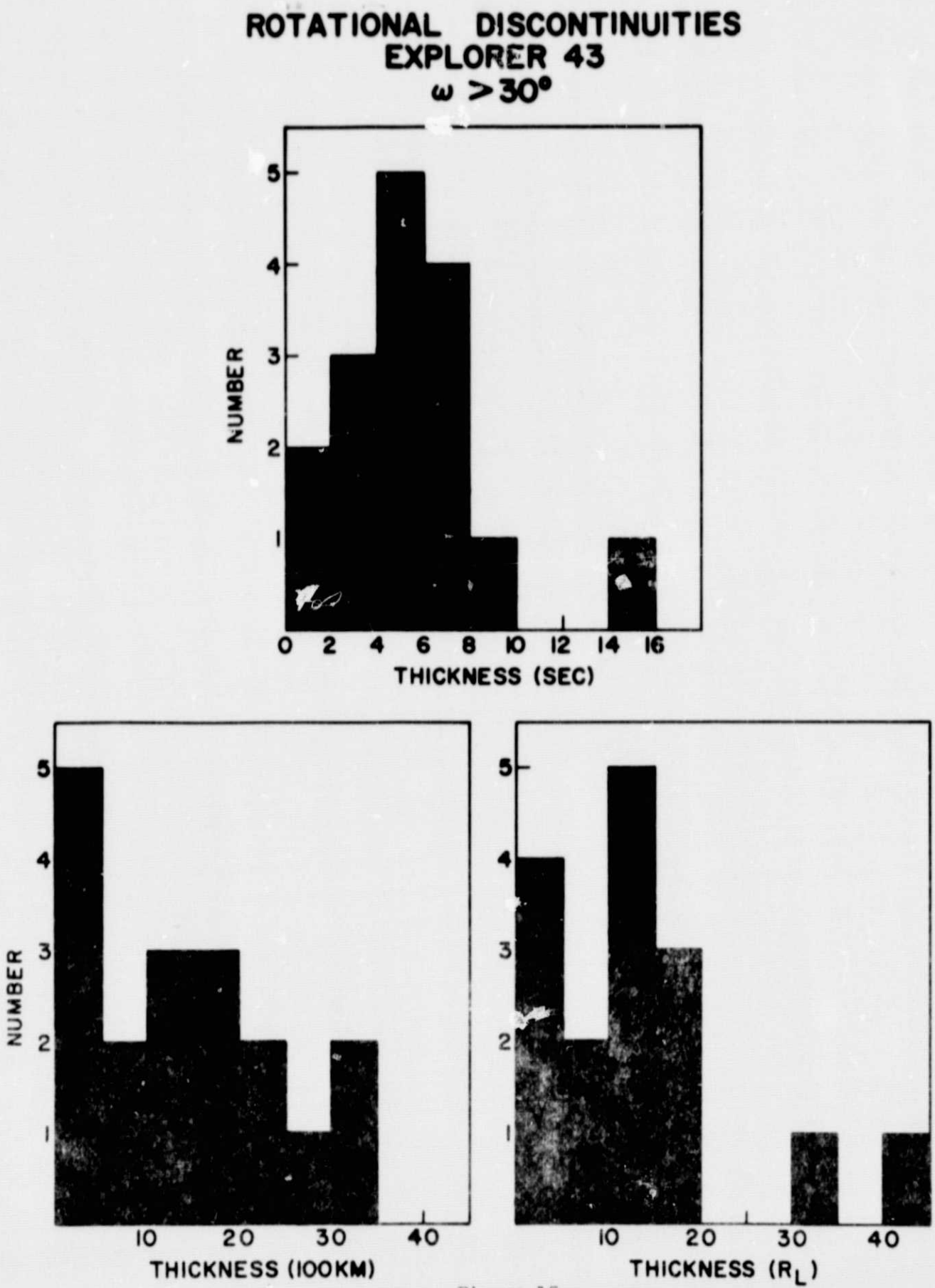
ROTATIONAL DISCONTINUITIES
EXPLORER 43
ω >30°
NUMBER
THICKNESS (SEC)
THICKNESS (100KM)
THICKNESS (R_L)

Figure 15